JFAPBC (2005) 6:54-63
DOI: 10.1361/154770205X76303

1547-7029 / $19.00

Evaluation of a Leaf Spring Failure

C.K. Clarke and G.E. Borowski

(Submitted July 18, 2005; in revised form August 31, 2005)

The determination of the point of failure during an accident sequence of a rear leaf spring in a sport utility vehicle is presented in terms of fracture surface analysis and residual-strength estimates. Marks at the scene of the accident pointed to two possibilities for the point of failure: marks in the roadway at the start of the accident sequence and a rock strike near the end of the sequence. Evidence from rust and chemical contamination on the fracture pointed to the spring having been cracked in half prior to the accident. Extensive woody fracture and secondary cracking at the midplane of the spring was evidence for segregation and weakness in the spring. Stress estimates for the effect of both the weakness and prior cracking on the residual strength of the spring revealed reductions in strength of the spring that could produce fracture at the start of the accident sequence. The point of failure of the spring was placed at the start of the accident sequence.

Keywords: fracture mechanics, leaf spring failure, leaf spring stress analysis, woody fracture

Introduction

Identification of the point in time that a fracture occurs can be crucial in the reconstruction of an accident, particularly those involving vehicles. Evidence to identify the point in time of the failure can be found in different forms. The failure analysis presented in this paper made use of evidence for fracture surface contamination, unusual fracture morphology, stress analysis, and fracture mechanics to identify the point in time in an accident sequence of an automotive leaf spring failure. This work grew out of a larger investigation of a loss-of-control accident in which both a rear leaf spring and a rear axle were found broken after the accident. The obvious question was, "Did one of these components cause the accident, or were they the result of the accident?" A brief description of the accident follows.

Written reports, statements, and a measured map of the scene showing road mark and object locations reveal that the vehicle was traveling at approximately 60 to 70 km/h on a dirt road when a clicking noise was heard upon entering a gentle curve that ran downhill. The vehicle drifted to the left side of the road, then turned sharply to the right across the road and sharply back to the left. The vehicle then ran along the left edge of the road until it struck large rocks. Impact with the rocks was along the left side of the vehicle. The vehicle rolled at this point, according to some reports. The right rear wheel was found fully inflated in the middle of the road near the start of the accident sequence. Subsequent inspection revealed that the left rear spring was broken at the forward eye and was bent sharply upward at the rear end of the first helper leaf.

The following day, investigators at the accident scene found marks in the dirt road that were well preserved and were the basis for mapping the path of the vehicle. They also found marks consistent with the right rear brake backing plate contacting the dirt roadway early in the sequence. A geological analysis of dirt found embedded in the backing plate determined that it was consistent with the roadbed materials, which were primarily limestone and sand. Soil outside the roadbed was different and was primarily red sand with little limestone. Quantitative analysis of the material in the backing plate was close to that of the roadbed materials and distinctly different from the surrounding terrain. No marks from a single rolling or bouncing tire in the road were reported further down the roadway.

Examination of the vehicle revealed the presence of rotating tire rub marks in the aft end of the left rear wheelwell and rotating tire rub marks in the forward end of the right rear wheelwell. Rupture of the left rear spring at the forward attachment would allow the left side of the axle to pivot to the rear about the right side spring-to-axle connection. Thus, the left wheel would rub at the rear of the wheelwell,

C.K. Clarke, Metallurgical Consulting, 1146 Leroy Stevens Rd., Suite A, Mobile, AL 36695. **G.E. Borowski,** Borowski Engineering, 1420 Polaris Dr., Mobile, AL 36693. Contact e-mail: kclarke@metalconsult.com and geborowski@yahoo.com.

and the right wheel would rub forward into the wheelwell. The pivoting axle will produce a steering effect independent of the front wheels and lever the right rear wheel into the frame rail. Because the tire rub marks show that the right rear wheel was as yet still rotating and unbroken, the left rear spring broke first. Therefore, the rest of the investigation was focused on the failure of the left rear spring.

Spring Fracture Evaluation

Fracture of the spring occurred at the formed forward eye, as shown in Fig. 1. Comparison of the eye with unbroken springs revealed that it had somewhat unwrapped prior to the failure. The position of the two broken ends in Fig. 1 exaggerates the prior deformation. Striking features of the fracture were the presence of extensive secondary cracking at the midplane, the stepped nature of the fracture, and "woody fracture" on the stepped surface parallel to the spring surface. Figure 2 shows the overall fracture with the secondary cracking. The woody fracture was difficult to photograph because it faced the spring surface. Damage to the opposite half of the fracture prevented much work with it. Permission to cut the eye half of the fracture for better examination was never granted.

Figure 2 shows a distinct division of the fracture along the midplane. Stereomicroscopy revealed a step in the fracture surface at this location, with deep secondary cracking along 73% of the midplane. An old, rusty crack was also observed along the outside surface over most of the width of the spring. This old crack (arrows) is shown in a higher-magnification view in Fig. 3. The outer half of the fracture with the old crack was also observed to have rust, compared to the inner half. Figure 4 shows the inside fracture surface opposite that in Fig. 3. The outside surface clearly shows areas of rust, particularly along the old crack. The inner half of the spring fracture

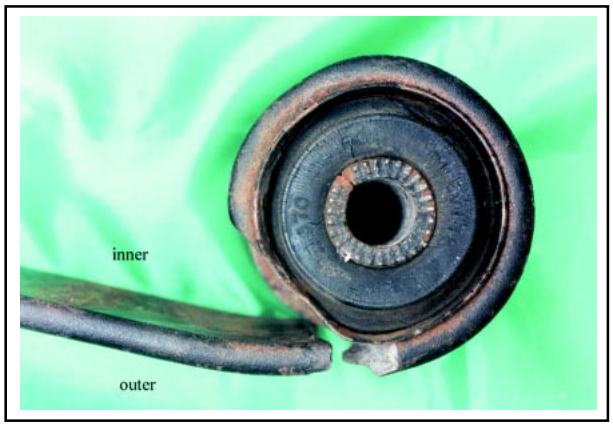

Fig. 1 *The broken halves of the spring have been placed together in a manner exaggerating the opening of the eye before rupture.*

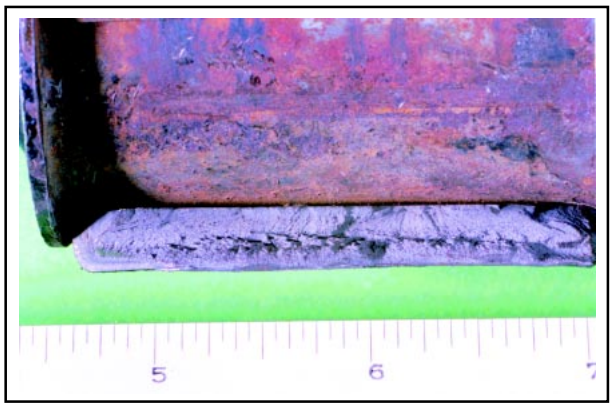

Fig. 2 *The spring half of the fracture has deep secondary cracking along the midplane.*

Fig. 3 *The outer half of the fracture surface was observed to have rust in places. The old crack (arrows) along most of the outer surface is clearly rusted.*

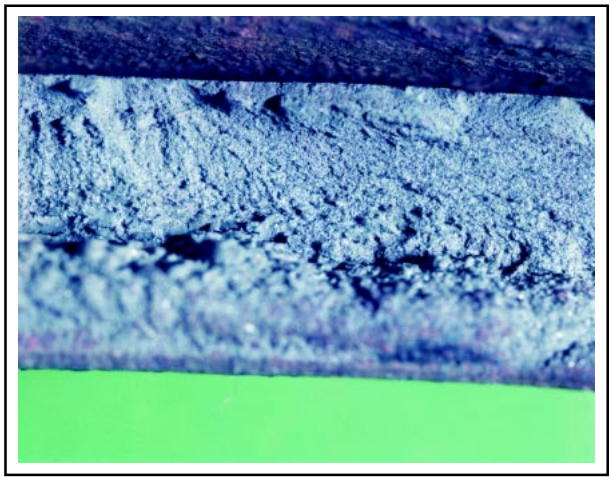

Fig. 4 *This area of the inner half of the fracture across from the area in Fig. 3 is clear of rust.*

was devoid of rust. Figures 3 and 4 were taken under identical conditions using Ektachrome 4 × 5 sheet film (Eastman Kodak Co.) in order to faithfully record the color differences and serve as the basis for color printing.

A scanning electron microscope (SEM) was used to examine the fracture on the eye at higher magnifications. Examination of the midplane fracture was difficult because the midplane fracture surface faced the surface of the spring itself. Such a geometry creates signal detection problems, particularly for X-ray analysis.[1] However, significant results were achieved by repeated repositioning of the spring eye.

The SEM fractograph of the spring eye fracture in Fig. 5 clearly shows the midplane cracking and old crack along the outside diameter (OD) surface (arrows). This old crack exhibited features indicative of a corroded surface, as can be seen in Fig. 6. Fracture between the old crack and the midplane was also rusted but less so than the old crack. The fracture mode in the old crack was difficult to see because of corrosion and physical damage. However, a few small areas were clear enough to reveal uniform, very small microvoids. Fracture between the old crack and the midplane was also by microvoid coalescence, but the void size was duplex with large and small microvoids. The fracture was also rougher.

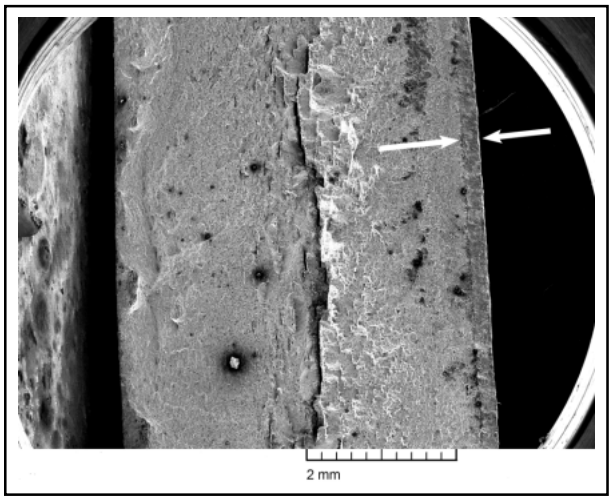

Fig. 5 *This area of the spring eye half of the fracture clearly shows secondary cracks at the midplane and an old crack (arrows) at the outside surface.*

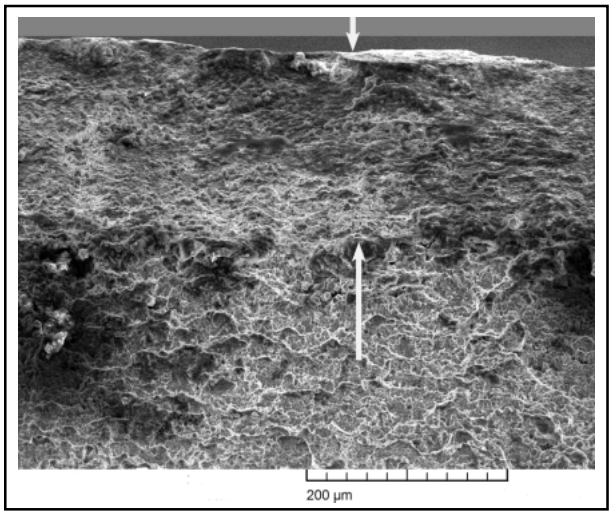

Fig. 6 *More detail of the old crack (arrows) shows a rusted surface compared with fracture next to it.*

X-ray spectroscopy of the old crack in the SEM revealed unusually high peaks for oxygen, silicon, calcium, chlorine, sulfur, and aluminum. Figure 7 shows one of the X-ray spectra from the old crack.

Calcium, silicon, and aluminum are contamination elements, because they should not be present at the observed concentrations on a 5160 steel fracture surface. The geological report revealed calcium carbonate, alumina, and, to a lesser extent, silica were a major portion of the road material. Chlorine was not reported in the roadbed analysis, and roads are not salted for ice where the vehicle was driven. An

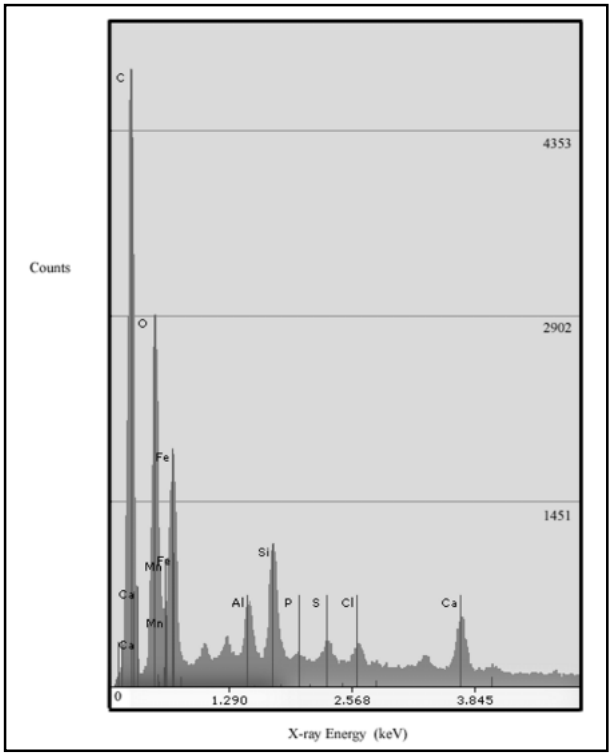

Fig. 7 *X-ray spectra from the old crack yielded high levels of carbon and oxygen. The other elements—calcium, aluminum, and silicon—are consistent with the road material. Chlorine can only be explained by ocean shipment.*

obvious source for chlorine in this case was the known transport of the vehicle by an ocean-going ship. The high oxygen level is consistent with corrosion. The source of the sulfur is not known at this time.

Figure 8 shows one area of "thumbnail-shaped" crack origins on the inside diameter (ID) surface. Chevron marks can be seen emanating from smaller thumbnails in Fig. 4. These regions were at an angle to the fracture and probably constitute a slow tear or low-cycle-fatigue-type feature. They triggered the final rupture of the spring.

Figure 9 shows a representative area of fracture approximately halfway between the inside surface of the spring eye and the midplane fracture. This fracture surface is perpendicular to the long axis of the spring. Extensive intergranular fracture mixed with microvoids was observed in this region of the fracture. Grain boundaries in steel are stronger than the grains at normal operating temperatures,[2] unless an element or compound develops on the boundaries and weakens them.[3-5] Steels with this problem often exhibit lower toughness and are more sensitive to shock or rapid loading. There are a number of phenomena that can produce this problem. Leaf springs are normally hot formed, quenched, and tempered. Prolonged cooling through or tempering at certain temperature ranges can produce temper embrittlement that can result in the observed intergranular fracture. Under the proper conditions, sulfides can also penetrate grain boundaries as thin films and produce intergranular fracture at elevated temperatures.

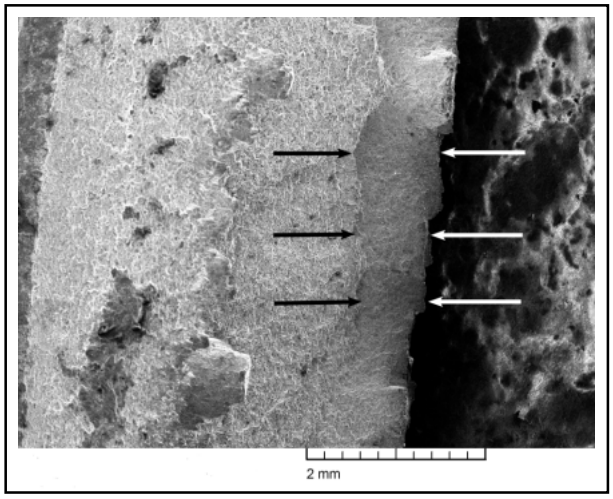

Fig. 8 *Chevron marks were observed propagating from the edges of these thumbnail areas (arrows) at the ID edge.*

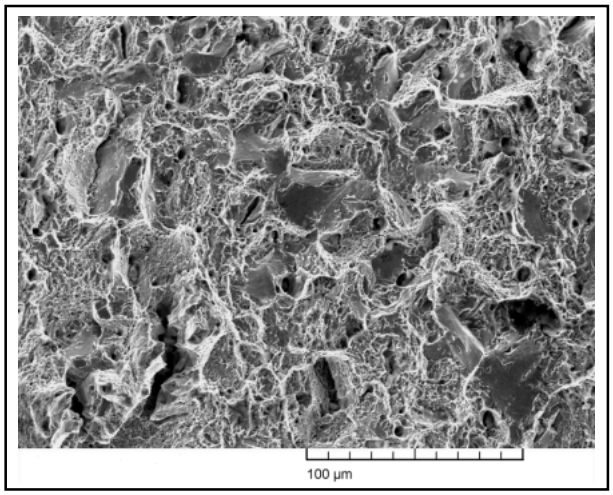

Fig. 9 *This fracture area is approximately halfway between the inside spring surface and the midplane fracture. It is composed of a mixture of intergranular fracture (smooth areas) and microvoids.*

The midplane fracture referred to in this report is an area of "woody"[6,7] secondary fracture in the middle of the spring fracture that is parallel to the plane of the spring and perpendicular to the main fracture. Extensive secondary midplane fracture of this type in a bending failure is unusual, because tensile transverse stresses (across the spring thickness) are not expected, and shear stresses in this area are very low compared to expected steel strength. Therefore, this type of fracture is indicative of a weakness in the midplane.[8,9] Weakness at the midplane in bending can seriously weaken the spring. Woody fracture at the midplane is shown in Fig. 10. One area in Fig. 10 reveals a smooth region that was caused by rubbing or repeated contact (arrows). X-ray spectra from the rubbed surface in Fig. 10 exhib-

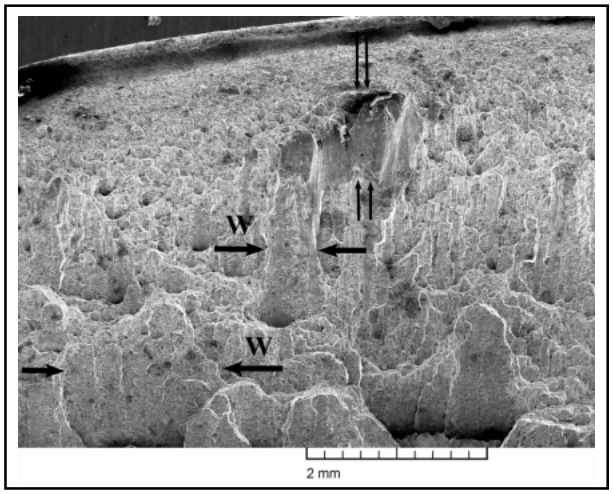

Fig. 10 *The fracture has been tilted to show woody fracture (W). Double arrows point to rubbing damage on woody, secondary fracture.*

ited strong peaks for silicon, carbon, oxygen, aluminum, and chlorine. Because the electron beam for X-rays was focused only on the smooth, rubbed surface and the fracture was solvent cleaned, the elements present in these strong peaks must come from contamination ground into the rubbed surface.

The woody area is an unusual fracture mode and is the result of banded inclusions and possible elevated-temperature problems. Woody fracture regions on this specimen were observed to be areas of decohesion of flat, elongated sulfide inclusions with regions of very fine microvoids in the broken ligaments. Bands of intergranular fracture were observed to be mixed in with the fracture. Figure 11 shows both of these morphologies together. X-ray analysis of the intergranular fracture area and the woody area in Fig. 11 revealed strong peaks for carbon, oxygen, silicon, aluminum, and chlorine. For comparison, X-ray analysis of the clean, inboard half of the fracture revealed only a small peak for silicon in addition to the normal peaks for iron, manganese, and chromium.

Exemplar Tests

Two exemplar springs from a vehicle of the same make and model were purchased and tested. The springs were pulled in tension using a horizontal hydraulic test machine. Rear shackles from the exemplar vehicle were used to load the rear ends of the springs. Clevis plates were machined and used to load the front ends. Both springs were pulled to rupture by pulling along the spring axis. Loading was interrupted at 17,800 and 35,600 N to examine the eyes. The eyes were observed to have opened or unwrapped approximately 10 mm at 17,800 N, and this opening stayed approximately the same at 35,600 N. (This is probably the same unwrap as the accident spring.) Rupture occurred at 47,700 and 48,800 N.

Both springs fractured at the forward eye in the same location and fashion as the accident spring. Spring B fracture exhibited more of the woody fracture and secondary cracking at the midplane than spring A. Figure 12 shows some of the woody fracture on spring B.

Fracture surfaces were cut from the springs for easier microscopic examination and for metallography. This provided for a more complete examination than was possible for the accident spring.

Both springs exhibited a distinct band on the fracture surface along the OD side in the same location where the existing oxidized crack was observed in the accident spring. Figure 13 shows this band on

Fig. 12 Woody fracture at the midplane can be seen in this view of fracture in exemplar spring B.

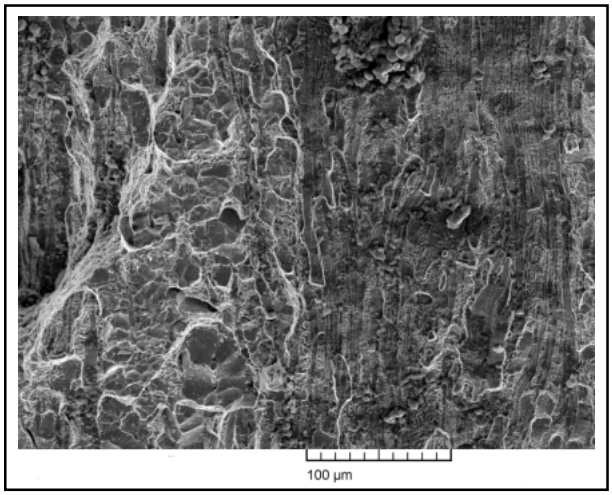

Fig. 11 This higher-magnification view of the woody secondary fracture shows that intergranular fracture is also associated with it.

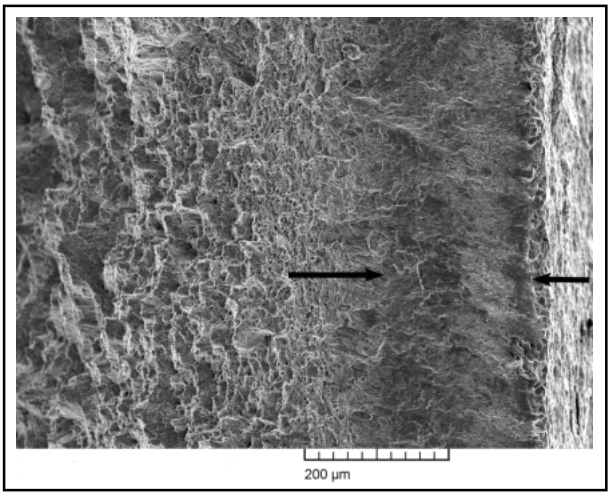

Fig. 13 An outside rim (arrows) was observed in the fracture of exemplar spring B. This is the same location as the old crack in the accident spring.

the exemplar spring B, where it was more pronounced. Fracture to the inside of the band was rough and consisted of large and small microvoids. Much of the fracture in the band was damaged, but small, protected areas in the band revealed very fine microvoids, as seen in Fig. 14.

Fracture in the area on the ID side and toward the midplane appeared faceted under a low-power microscope. The SEM examination revealed mixed intergranular fracture and microvoids. The amount of intergranular fracture increased toward the midplane. Fracture morphology in this region was very similar to that observed in the accident spring.

Woody fracture in the B spring was very similar to the accident fracture. Both midplane fracture surfaces (accident and exemplar) exhibited small damaged areas on the woody fracture. Figure 15 shows an area of woody fracture with surface damage similar to that seen in the accident spring. However, higher-magnification examination revealed evidence for a single contact compared to repeated rubbing observed in the accident fracture. X-ray spectra from this damaged area on the exemplar fracture yielded none of the contamination observed in the accident spring.

The exemplar fractures were cut and removed from the spring eye for better SEM examination. These fracture surfaces provide better conditions for analysis of the midplane fracture than has been possible on the accident fracture. The same mix of intergranular fracture and woody fracture was observed in the B spring fracture. Figures 16 and

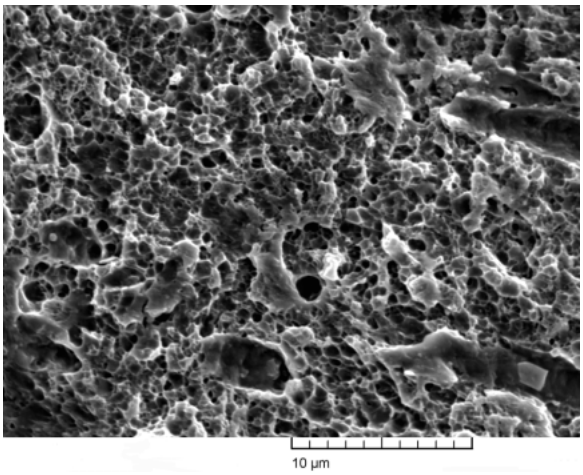

Fig. 14 *Very fine equiaxed microvoids could be observed in undamaged areas of the OD band fracture. While microvoid formation is a ductile or plastic mechanism, the macroscopic ductility or toughness of this type of fracture with very fine microvoids is low.*

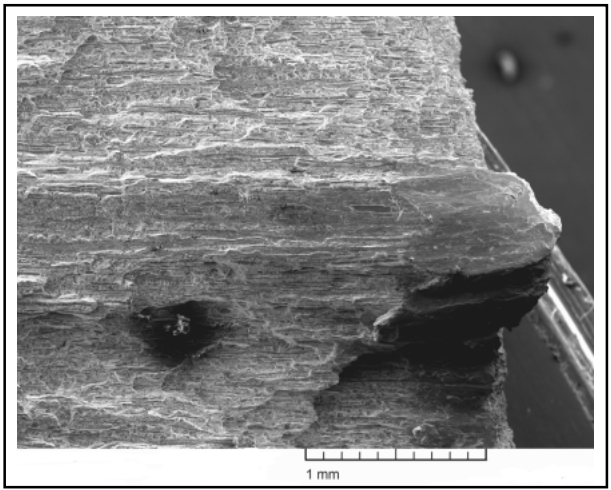

Fig. 15 *Damaged areas were observed on the woody fracture in the B spring, as in the accident spring.*

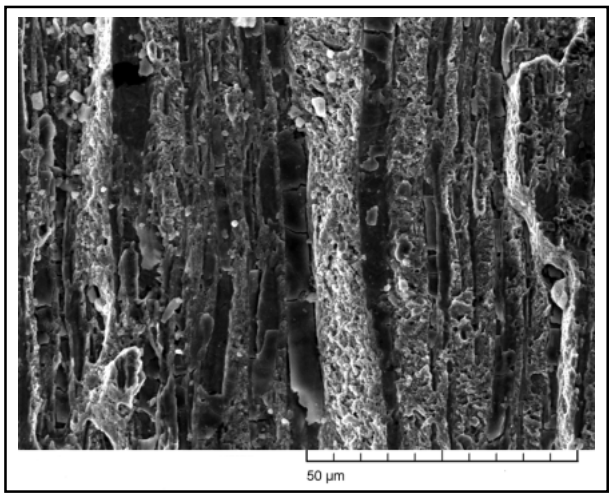

Fig. 16 *An area of woody fracture. The X-ray map of Fig. 17 can be superimposed over this micrograph.*

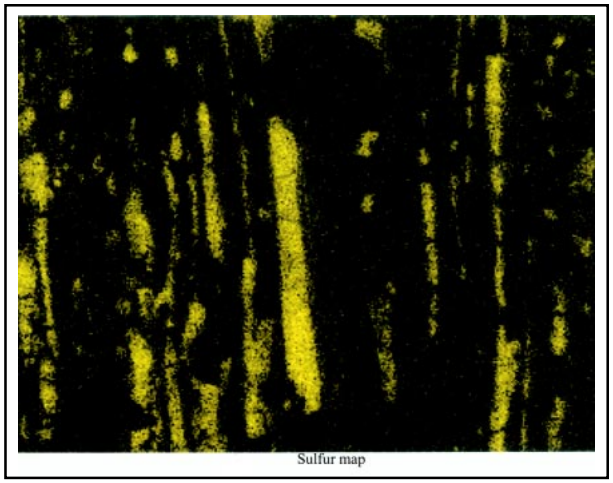

Fig. 17 *This map of the area in Fig. 16 was made with sulfur X-rays only. This clearly shows the role of sulfur inclusions in the midplane woody fracture.*

17 show that the woody fracture is associated with manganese sulfide inclusions. Figure 16 shows an area of woody fracture. Figure 17 is a map of the sulfur X-ray signals coming from the same area as in Fig. 16. Sulfur coincides with obvious inclusions and some that are not obvious. Manganese also yielded the same map. While the inclusions are very fine, their planar extent is substantial.

Cross sections were cut through the woody fracture. Figure 18 shows the midplane cracking in spring B. Optical microscopy revealed the midplane cracking to be associated with banding in the microstructure. Figure 19 shows the tip of the midplane crack in spring B to be associated with a white band with elongated inclusions. (Heavy etching to bring out the band obscured the inclusions.) Numerous fine, elongated sulfide inclusions were observed in these bands.

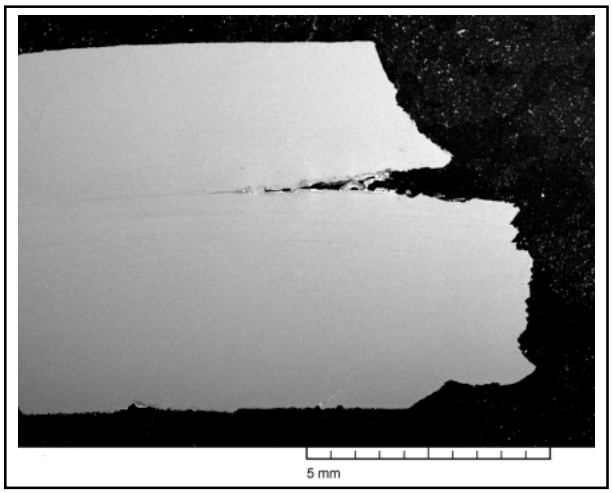

Fig. 18 Cross section of the fracture in spring B. The midplane fracture is very pronounced.

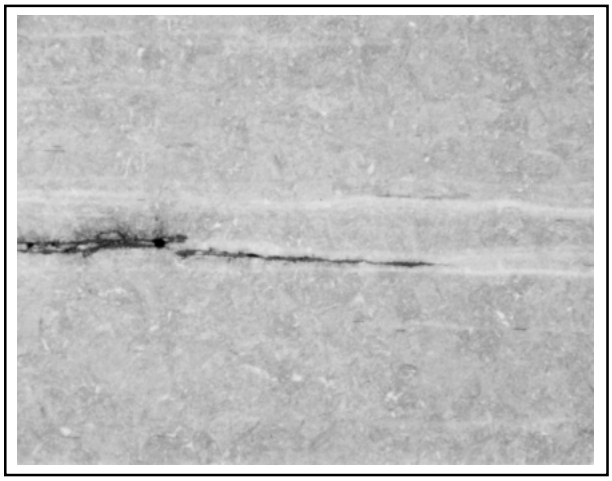

Fig. 19 The tip of the midplane crack in spring B follows a white band.

X-ray spectroscopy in the SEM failed to reveal any significant chemistry differences in these white banded areas. Carbon, chromium, sulfur, phosphorus, and manganese were analyzed for any systematic variation, and none was observed. Sulfur and manganese were again found to be associated with the elongated inclusions observed in the cross sections and with woody areas on the midplane fracture.

Stress Analysis

Stress calculations were performed to estimate the reduction in strength in the spring resulting from cracks existing before the accident and the midplane segregation. Exemplar spring test data were also used to provide a basis for estimating the reduction in strength. The reduction-in-strength estimates were then used to determine if normally expected dirt road forces in the absence of a large rock strike were adequate to rupture this spring. Finite-element stress analysis was used to study the existence of transverse tensile stresses at the location of the fracture.

A limited finite-element analysis using the commercial finite-element code ALGOR (ALGOR, Inc.) was conducted on the spring eye stress conditions in order to examine the transverse stresses. The leaf spring was secured directly to the vehicle frame at the forward end and through a shackle assembly at the aft end. This arrangement is shown in Fig. 20. A rubber grommet with a steel outer sleeve and an inner steel bolt sleeve, both bonded to the rubber, was placed in each eye so that the assembly would not slip. The bolt sleeve ends were serrated so that they would not rotate against the

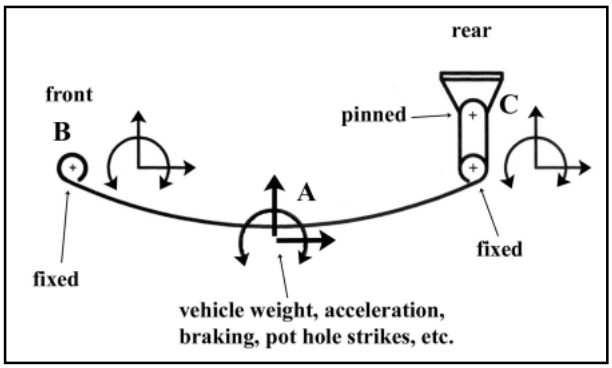

Fig. 20 Reaction forces on the spring eyes in the vehicle are complex. Both spring eyes can develop moments through the rubber grommet. The link at "C" is free to rotate. Longitudinal forces develop at "A" from both direct longitudinal forces and moments from the tire to the spring.

frame. The ALGOR program modeling this arrangement revealed that the rubber properties had a significant effect on the spring stresses at the point of failure. The program also predicted higher stresses at the end of the first helper leaf than at the spring eye. This is consistent with the Society of Automotive Engineers' spring-design manual.[10] Stresses at the spring eye should be low, according to the spring manual. Different cases were run with different assumed rubber properties, because the actual properties were not known. These cases revealed that transverse tensile stresses did occur at the midplane, and their magnitude depended on the compliance of the rubber and the fixity of the bolt collar. These calculations help to explain the tensile nature of the woody fracture and provide a source of service stresses that could produce delamination.

Residual-strength calculations were made with longitudinal forces only, because they simplified the calculations, and pull test data were available for comparison. Use of longitudinal forces only does provide a meaningful analysis of the spring failure, because reaction forces at the spring eye from pothole strikes and moments from the tire-axle housing-spring connection produce longitudinal forces. Figure 21 shows these forces on the spring eye.

The first strength calculation involved the longitudinal force required to produce permanent deformation in the eye from a pull test. (This would be observed as unwrapping or opening of the eye.) Both exemplar springs were observed to have deformed at 17,800 N axial force. The stresses must exceed the proof or yield stress in order for this to occur. The yield stress is expected to be at least 1240 MPa for these springs. An undelaminated spring only reaches a maximum outer surface stress of 1120 MPa with 17,800 N pull (1240 MPa minimum yield), while a spring delaminated to the extent observed in the accident vehicle would reach outer surface stress levels well above yield (2530 MPa, calculated elastically). (Delamination reduces the moment of inertia, which in turn elevates stresses.) Thus, the premature deformation of the exemplar springs, which had midplane segregation, can be explained. Midplane segregation definitely reduces the strength of the springs in this application.

The next step was to estimate the reduction in strength produced by the old OD crack. This estimate was based on published stress-intensity (K_{Ic}) data. Published data for lower-carbon steels heat treated to similar strength levels as the spring reveal a critical K_{Ic} range of 50 to 110 MPa$\sqrt{m}$[11] Data for 5150 steel place the K_{Ic} at 82 MPa$\sqrt{m}$ or less.[12] An estimate of 65 MPa$\sqrt{m}$ or less is appropriate for 5160. (Plane-strain conditions did exist in the spring.) These data, plus the crack depth measurements for the old OD crack, produced an estimate of 1460 MPa for an outer fiber bending stress required for spring fracture. The calculated outer fiber (or outer surface) bending stress estimated for fracture in the presence of the small OD crack is at or below the expected tensile strength for the spring. Steels with substantial ductility (as evident in the subject spring due to its "unwrapping" prior to rupture) will readily exceed the tensile strength (by elastic calculation) in bending before rupture. This analysis indicates that the strength has been reduced when compared to the nominal properties. Any delamination in the spring would raise the stresses and result in unstable fracture at even lower force levels. (The observed delamination would double the stresses.)

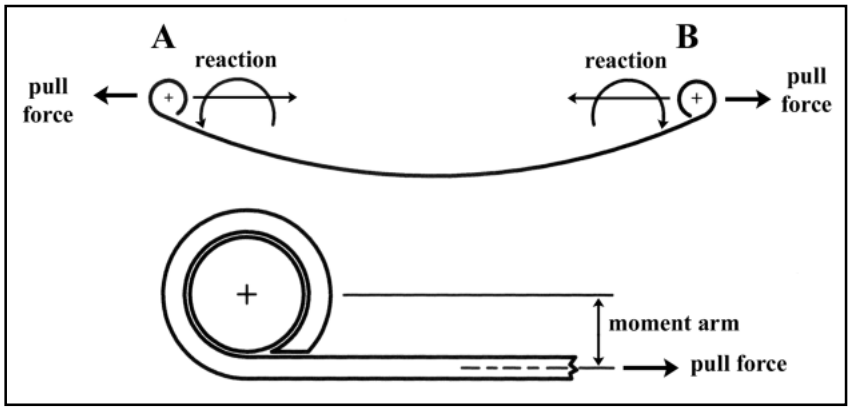

Fig. 21 Reaction forces in the spring eyes were simpler by the very nature of the pull test. Spring curvature was neglected because the spring straightened out early in the test. Bending stresses were based on the spring eye radius.

The longitudinal force required to produce the fracture initiation stress predicted by fracture mechanics was estimated by elastic bending calculations. While the stresses are above the yield stress, this approach normalizes the stresses on an elastic basis to provide a

reasonable measure of reduction in strength. (An elastic-plastic analysis was beyond the scope of the project.) Using this approach, the force to reach 1460 MPa was estimated to be 23,000 N for no delamination and 10,200 N for the observed delamination in the accident spring. Using 48,200 N pull to failure from test results on exemplar springs yielded a 52 to 79% reduction in spring strength. These numbers demonstrate the serious reduction in strength possible for both the small crack and the delamination. (Small cracks in hard or high-strength steels are well known for severely reducing the strength.) Evidence of the outer half being cracked for some time indicates that the reduction in strength did in fact occur.

The midplane segregation leading to delamination would be expected to arrest the running crack from the outside surface, and it did. This would leave the spring weakened but intact. Rubbing at the midplane demonstrates that this arrest did occur. Residual strength for this condition was estimated by assuming the spring was cracked halfway through. The calculated maximum elastic outer fiber stress at failure for the exemplar springs was used as the failure criterion. A 12,900 N pull to rupture was estimated using this approach. This is a 73% reduction in strength over the exemplar springs, or 0.72 g forward deceleration for a 17,800 N vehicle. Accelerations of 0.72 g or less are in the range of reasonably expected forces for a vehicle traveling on dirt or unimproved roads. Final rupture forces for the spring were probably lower still. Thumbnail regions were observed at the ID surface on the accident and exemplar springs at approximately 45° to the spring surface and to the rest of the ID half of the fracture. These thumbnail regions are at least plane-stress stable tear features. Once they reached a critical length, plane-strain unstable rupture occurred. The toughness of the ID half of the spring was less than that of the OD half because of the extensive presence of intergranular fracture, which is evidence for embrittlement. Therefore, the combination of a stable tear and dynamic loading probably further reduced the final longitudinal rupture force below 0.72 g.

Discussion

There was considerable evidence that the spring was cracked for some time before the accident:

- A long, rusted crack was observed on the OD surface.
- A significant presence of chlorine and calcium (along with other elements) was found in the OD crack and the midplane crack. Chlorine, in particular, could only be explained by prior travel on an ocean-going ship.
- Rust was observed on the OD half of the fracture but not on the ID half.
- Rubbing damage was observed locally on the midplane fracture.

Stress calculations to estimate the effect of the prior cracking yielded residual-strength levels in the spring that could be reasonably expected in travel over a dirt road. Thus, conditions for spring rupture existed prior to the start of the accident sequence. Location of the point of rupture of the spring should therefore be placed at the beginning of the accident sequence, because the stresses for rupture were present at that point.

Location of the rupture of the spring at the start of the loss of control is consistent with other evidence in the accident. Wheel scrub marks in both wheelwells are consistent with a rolling tire. Fracture of the spring in a rock strike would produce less than a quarter of a revolution, because the impulse would be on the order of milliseconds. This was not consistent with marks in the left rear wheelwell. A set of marks in the road early in the loss of control was identified with the backing plate, thus locating the axle failure early in the sequence. Based on this sequence, the spring failure must have preceded the axle failure.

Midplane segregation in the spring steel appears to have played a significant role in the failure of the spring. Failure of the spring at the eye is not the normal location for automotive leaf spring failures. Stresses are higher at the edge of the first helper leaf. The arrangement of the forward spring to the frame attachment appears to have created a situation in which across-the-thickness tensile stresses could develop. The residual-stress distribution at this location is unknown but could easily be tensile. Any opening of the midplane along the banded regions would weaken the spring. This problem, outside of preexisting cracks, could move the point of expected failure to the spring eye. Premature opening of the exemplar eyes in longitudinal pull tests, as well as

both exemplar springs failing at the forward eye, can also be explained by the midplane segregation problem.

Conclusions

The failure analysis yielded the following conclusions:

- The presence of sulfur segregation at the midplane weakened the spring.
- The spring was cracked for some time in advance of the accident.
- The prior cracking in the spring was extensive enough to reduce the strength of the spring to the point where normal dirt road forces were adequate to produce rupture.
- Marks in the wheelwells and on the road surfaces were consistent with and support rupture of the spring at the start of the accident sequence.
- The rock strike possibility was ruled out because forces adequate to rupture the spring were present well in advance of the rock strike, and wheelwell marks were not consistent with short-duration forces expected from a rock strike.

References

1. J. Goldstein et al.: *Scanning Electron Microscopy and X-Ray Analysis,* 3rd ed., Kluwer Academic/Plenum, New York, NY, 2003, pp. 476-79.
2. A.J. Tetelman and A.J. McEvily: *Fracture of Structural Materials,* John Wiley, New York, NY, 1967, pp. 105-07.
3. R.W. Hertzberg: *Deformation and Fracture Mechanics of Engineering Materials,* 3rd ed., John Wiley, New York, NY, 1983, pp. 258-59.
4. H.E. McGannon, ed.: *The Making, Shaping, and Treating of Steel,* 8th ed., U.S. Steel, Pittsburgh, PA, 1964, pp. 355-56.
5. C.L. Briant and S.K. Banerji: "Intergranular Failure in Steel: The Role of Grain Boundary Composition," *Int. Met. Rev.,* 1978, *23*(4), pp. 164-99.
6. D.A. Moore, K.F. Packer, A.J. Jones, and D.M. Carlson: "Crankshaft Failure and Why It May Happen Again," *Prac. Fail. Anal.,* 2001, *1*(3), pp. 63-72.
7. *Fractography and Atlas of Fractographs*, vol. 9, *Metals Handbook,* 8th ed., American Society for Metals, Metals Park, OH, 1974, pp. 29-30.
8. J.C.M. Farrar and R.E. Dolby: "Lamellar Tearing in Welded Steel Fabrication, The Role of Sulfide Inclusions," *Sulfide Inclusions in Steels*, J.J. de Barbadillo and E. Snape, ed., American Society for Metals, Metals Park, OH, 1975, pp. 252-68.
9. A.J. DeArdo and E.G. Hamburg: "Influence of Elongated Inclusions on the Mechanical Properties of High Strength Steel Plate," *Sulfide Inclusions in Steels,* J.J. de Barbadillo and E. Snape, ed., American Society for Metals, Metals Park, OH, 1975, pp. 309-37.
10. *Manual on Design and Application of Leaf Springs*, SAE HS 788, Society of Automotive Engineers, Warrendale, PA, April 1980.
11. R.W. Hertzberg: *Deformation and Fracture Mechanics of Engineering Materials,* 3rd ed., John Wiley, New York, NY, 1983, p. 411.
12. *Fatigue and Fracture,* vol. 19, *ASM Handbook,* ASM International, Materials Park, OH, 1996, pp. 622, 625.